Available online at www.sciencedirect.com

ScienceDirect

materialstoday: PROCEEDINGS

Materials Today: Proceedings 3S (2016) S153 – S158

Proceedings of the International Conference on Diamond and Carbon Materials

Numerical modelling of polycrystalline diamond device for advanced sensor design

Arianna Morozzi[a,b,*], Daniele Passeri[a,b], Keida Kanxheri[b], Leonello Servoli[b], Silvio Sciortino[c], Stefano Lagomarsino[c]

[a]*Dipartimento di Ingegneria,Università degli Studi di Perugia, via Duranti 93, Perugia 06131, Italy*
[b]*INFN - Sezione di Perugia, via Pascoli 1, 06123 Perugia, Italy*
[c]*INFN – Sezione di Firenze, via G. Sansone 1, 50019 Sesto Fiorentino, Italy*

Abstract

Technology Computer Aided Design (TCAD) simulation tools are routinely adopted within the design flow of semiconductor devices to simulate their electrical characteristics. However, the device level simulation of diamond is not straightforward within the state-of-the-art TCAD tools. Physical models have to be specifically formulated and tuned for single-crystal CVD (scCVD) and polycrystalline (pcCVD) diamond in order to account for, among others, incomplete ionization, intrinsic carrier free material, dependences of carrier transport on doping and temperature, impact ionization, traps and recombination centers effects.
In this work, we propose the development and the application of a numerical model to simulate the electrical characteristics of polycrystalline diamond conceived for sensors fabrication. The model is based on the introduction of an articulated, yet physically based, picture of deep-level defects acting as recombination centers and/or trap states. This approach fosters the exploration and optimization of innovative semiconductor devices conjugating the capabilities of CMOS electronics devices and the properties of diamond substrates, e.g. for biological sensor applications or single particle detectors for High Energy Physics experiments.

Selection and Peer-review under responsibility of the chairs of the International Conference on Diamond and Carbon Materials 2014.

Keywords: TCAD; Numerical Modelling; Diamond

* Corresponding author. Tel.: +39-075-5853643; fax: +39-075-5853654.
E-mail address: arianna.morozzi@studenti.unipg.it

Selection and Peer-review under responsibility of the chairs of the International Conference on Diamond and Carbon Materials 2014.
doi:10.1016/j.matpr.2016.02.026

1. Introduction

Synthetic diamond exhibits electrical properties such as low dielectric constant and low losses, a high electrical carrier mobility and a wide electronic bandgap, fostering its application in electronics device and circuit design and fabrication. Within this framework, Technology Computer Aided Design (TCAD) simulation tools are routinely adopted, to simulate device and circuit electrical characteristics, as a response to external stimuli. However, the device level simulation of diamond is not straightforward within the state-of-the-art TCAD tools such as Synopsys© TCAD (Sentaurus). Physical models have to be specifically formulated and tuned for single-crystal CVD (scCVD) and polycrystalline CVD (pcCVD) diamond in order to account for, among others, incomplete ionization, intrinsic carrier free material, dependences of carrier transport on doping and temperature, impact ionization, traps and recombination centers effects.

In this work, we propose the development and the application of a numerical model to simulate the electrical characteristics of pcCVD diamond conceived for innovative sensors fabrication. The model is based on the introduction of an articulated, yet physically based, picture of deep-level defects acting as recombination centers and/or trap states. This approach fosters the exploration and optimization of innovative semiconductor devices conjugating the properties of diamond substrates and the functionalities of CMOS electronics devices.

2. TCAD diamond parameter setup

Diamond is a “novel” material for device-level numerical simulation tool; it is therefore necessary to add a new custom-defined semiconductor to the material library of the TCAD tool at hand, namely the Synopsys© Advanced TCAD Sentaurus. The main parameters of scCVD have been collected from literature and incorporated within the material definition. Among others, the wide band-gap, the exceptionally high carrier mobility, the high critical electric field, which make the diamond suitable for high-voltage and high-temperature applications [1, 2, 3].

However, aiming at “smart” electronics circuit and system design, the activation of dopants is an important issue that should be addressed for the application of diamond devices. It originates from the wide diamond bandgap, responsible for the large ionization energies of dopants in the material. The incomplete ionization still limits the number of carriers which can be introduced into the valance band with increasing dopant concentrations [4].
In this work an incomplete ionization model has been considered [5] by means of the following equations, which represent the concentration of ionized impurity atoms:

$$N_D = \frac{N_{D,0}}{1 + g_D \exp\left(\frac{E_{F,n} - E_D}{kT}\right)}, \quad for\ N_{D,0} < N_{D,crit} \qquad N_A = \frac{N_{A,0}}{1 + g_A \exp\left(\frac{E_A - E_{F,p}}{kT}\right)}, \quad for\ N_{A,0} < N_{A,crit}$$

where $N_{D,0}$ and $N_{A,0}$ are the donor and acceptor concentration, g_D and g_A are the degeneracy factors for the impurity levels and E_D and E_A are the donor and acceptor ionization (activation) energies. The $N_{D,crit}$ and $N_{A,crit}$ values were taken from [1]. The density-of-states for the conduction and valence bands (N_C and N_V) that influence the intrinsic carrier concentration have been set to $N_C = 5.0\times10^{18}$ cm^{-3} and $N_V = 1.8\times10^{19}$ cm^{-3} at 300K [3]. Boundary conditions and contact properties have to be set up as well. To this purpose, it should be mentioned that the electron affinity depends highly on the nature of the surface termination. In the experimental devices diamond surfaces are typically treated with an oxygen plasma (X_0 = 1.7 eV) or hydrogen plasma (X_0 = -1.3 eV) prior to contact realization [6].

With the aim of validating the parameter choice, in Fig. 1 is represented the comparison between the incomplete ionization model and the simulation results that have been obtained by means of steady-state simulations. Fig 2 shows a comparison between the simulated hole mobility as a function of the boron concentration and experimental results.

Once assessed the main parameters of the “new” material representing the scCVD diamond within the TCAD tools, a number of issues are still to be addressed for an efficient steady-state and transient (time-variant) analysis. In particular, the very low intrinsic concentration of the diamond, in the order of $n_i = 10^{-27}$ cm^{-3} at 300K, is unsuitable for typical TCAD solvers, because leads to numerical analysis issues. Possible strategies to cope with this issue are the following:

i. using an *artificial* doping concentration, i.e. a *quasi-intrinsic* material with a doping concentration $n_i = 1.0\times10^{11}$ cm^{-3} [1, 3].
ii. using the intrinsic, carrier free material approximation ($n_i = 0$ cm^{-3}) but considering the effect of trap levels and/or recombination centres within the bandgap, in order to simulate the effect of impurities and/or grain boundaries.

The first approach is the more widespread in literature. On the other hand the second approach is more physically grounded, and it is suitable to simulate an intrinsic device taking into account the effect of impurities and/or grain boundaries, that are peculiar of pcCVD diamond devices.

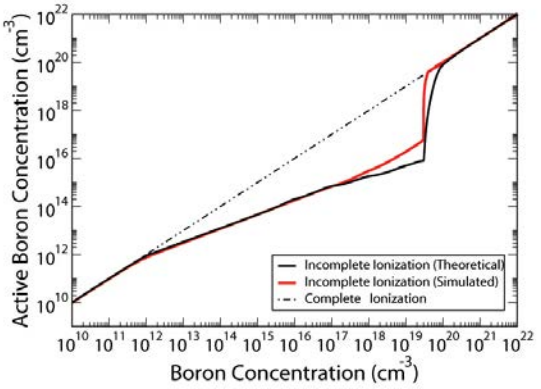

Fig. 1. Incomplete ionization of dopants (boron): comparison between simulated results and theoretical findings [1].

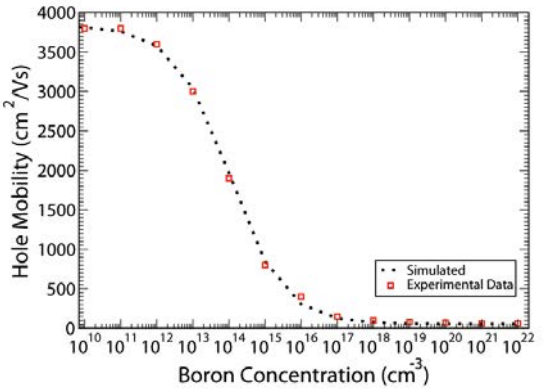

Fig. 2. Hole mobility vs. boron concentration: comparison between experimental results and simulated data [1].

3. The simulated structure: DC current analyses

In order to compare the simulation results with real measurements carried out on a diamond sample, a simple basic structure has been simulated, reproducing a 2D cut of a real device along two different axes (e.g. resulting in different contact distributions along the simulated domain) (Fig. 3). To begin with, we evaluated the electrical potential distributions of two orthogonal cross-sections. As illustrated in Fig. 4, the distributions are very similar, differing only within the very shallow surface region. Actually, since the bulk effects are dominating, we decide to adopt the cut (a) for sake of simplicity in terms of computational effort.

The effect of the doping concentration on the steady-state current calculation is very strong. Even a non-physical concentration of free carriers greater than zero has huge effect on the IV characteristic, which tends to increase as a function of the doping, as expected, but spanning over few tens orders of magnitude. This strong and non-physical dependence has suggested the adoption of a more realistic modeling scheme. Since, from the electrical point-of-view, impurities and grain boundaries act as trapping and/or recombination centers [7, 8], the idea is to model the diamond with the introduction of trap levels, in order to simulate the grain boundary effects. Within Sentaurus TCAD it is possible to add trap levels as well as defect bands that are composed of many levels and/or different energy distributions. For each level, it is possible to set the trap type (acceptor/donor), the energy level distribution function (single level, uniform, exponential or Gaussian band), the energy (position) within the band-gap, the trap concentrations, and the capture cross-sections for both carriers. The overall trap effect is typically described by the Shockley-Read-Hall statistics.

3.1. Single-Level Trap Modeling

We begin with considering an intrinsic diamond structure ($n_i = 0$ cm^{-3}) with a single defect level within the band-

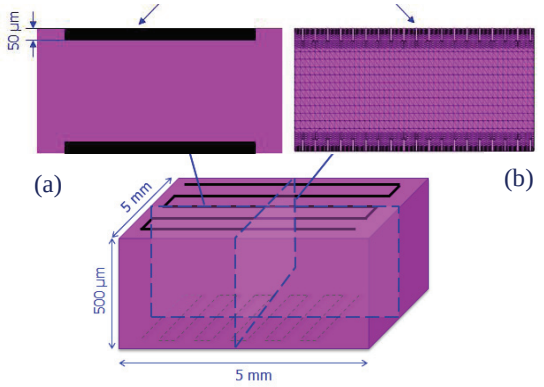

Fig. 3. The simulated 2D domains.

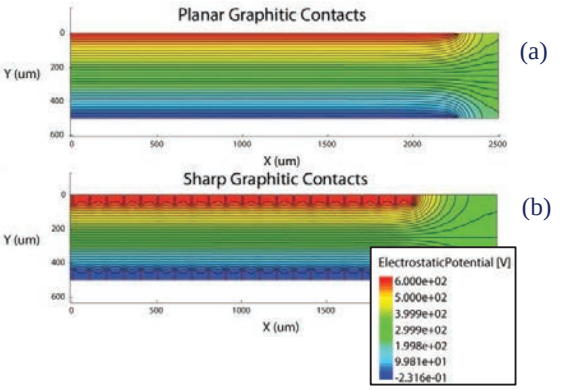

Fig. 4. Electric Potential distributions for two different sections.

gap and we calculate the steady-state current as a function of the trap position (Fig. 5). At a first glance, the behaviour of an acceptor level is dual to that of a donor level, irrespective of the position in the bandgap. Moreover if we consider a single trap level (acceptor or donor) in a diamond structure doped with boron atoms with $N_A = 10^{10}$ cm^{-3}, the effect of the shallow level (due to the doping) combines with that of the deep level (trap), resulting in an overall modification of the charge density and of the current (Fig. 6).

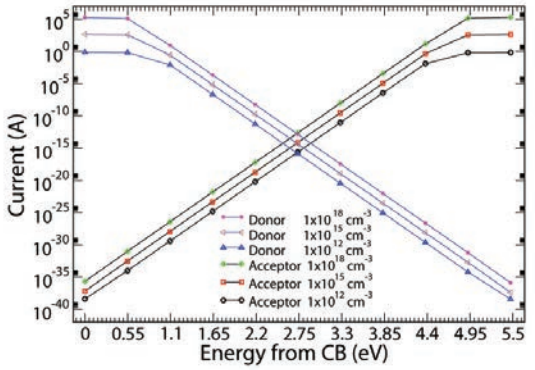

Fig. 5. Current as a function of the concentration and energy level for single acceptor and donor trap levels (intrinsic diamond).

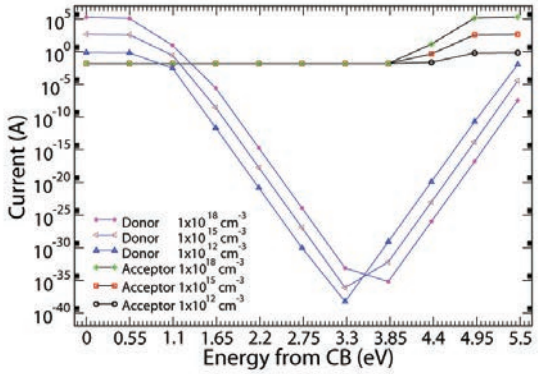

Fig. 6. Current as a function of the concentration and energy level for single acceptor and donor trap levels (doped diamond $N_A = 10^{10}$ cm^{-3}).

Fig. 7 shows the trap occupancy function depending on the energy of the defect level. A donor trap can actually entrap holes only if it is located very close to the conduction band (CB) edge while the acceptor trap can entrap electrons only if it is very close to the valence band (VB) edge. Is interesting to notice that the lower is the trap concentration, the higher is the probability that this trap is filled with carriers at energy away from the band edge. Indeed the trap concentration represents an upper limit of the maximum number of carriers that can be trapped. Trap type (acceptor or donor) and position (energy level) within the gap have a strong impact on free carrier densities, since the overall charge balance imposed by the Poisson's equation has to be satisfied. This in turns has a strong impact on the steady-state current flowing through the device when an external biasing voltage is applied.

3.2. Multiple-Level Trap Modeling

A more realistic modelling of the defects should consider the quite articulated picture of defect levels of a pcCVD diamond within the gap [7, 8]. We started by assuming a donor trap in few fixed positions and an acceptor trap level

that spans within the entire bandgap. As an example, a donor level with a concentration $N_T = 1\times10^{15}$ cm^{-3} at 1.09 eV from the CB has been considered, while the acceptor level spans from the CB to the VB with a pitch of 0.547 eV. For an acceptor trap level with concentration lower than the donor level concentration, the current value doesn't change even if the acceptor level position changes. On the other hand, for higher acceptor concentrations as long as the acceptor level is close to the CB, the current tends to decrease because these two traps tend to compensate each other. However when the acceptor trap is close enough to the donor trap the

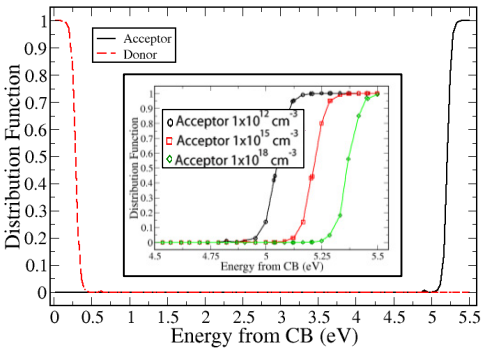

Fig. 7. Trap occupancy depending on the energy of the defect level. The inset shows a detail of the behaviour near the VB's edge.

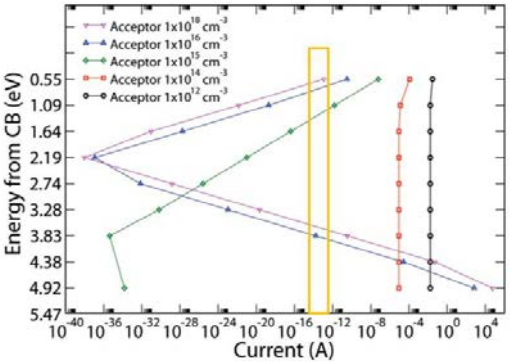

Fig. 8. DC current behaviour: fixed donor level at 1.09 eV from CB and $N_T = 1\times10^{15}$ cm^{-3}.

current starts increasing. As long as the acceptor level is close to the CB, the donor level prevails on the current behaviour. The current is reduced until the acceptor level reaches the midgap, after that the dominant effect is that of the acceptor trap and the current starts increasing (Fig. 8). A theoretical operation window (yellow box) with current value magnitude compatible with experimental findings is shown in Fig. 8. It is note worth that different parameterizations can lead to the same acceptable current values.

With this respect, it is worth mentioning as well that the aim of this modelling approach is to provide a robust parameterization, able to reproduce not only a particular operating condition (e.g. steady-state current for a fixed biasing), but also capable to reproduce the transient behavior with different stimuli and biasing conditions. Moreover, aiming at keeping the number of model parameters within a physically grounded scenario, we use the comprehensive bandgap model reported in [7] where is proposed a two-band model with one band (Band A) at midgap acting as a recombination centre and the other band (Band B) close to one of the band edges (either VB or CB edge). There is an experimental evidence supporting the picture of this two bands, a deep donor and a deep acceptor, with the Fermi level situated somewhere in between, so that the two distributions are charged at thermal equilibrium (de-pumped state).). We will refer to the deep acceptor distribution as band A and to the deep donor centre as band B, assuming that this trap is closer to the CB [9].

The experimental findings suggest that band A ranges from about 1.7 eV to 2.7 eV from the CB, where it has a maximum concentration, while band B is extended up to 1.7 eV from the CB [8]. A further shallow level has been introduced to simulate a more realistic trap dynamic behavior by considering the thermal emission of the electrons in the CB, that lead to persistent currents reported by experimental measurements as well. Eventually, a comprehensive reference model parameterization is reported in Table 1. The values of the capture cross-sections have been extracted from [10] while the trap densities have been used as fitting parameters for a better agreement with the experimental results.

4. Transient analysis

Time variant simulation have been carried out, aiming at evaluate the response of a pcCVD diamond to a minimum ionizing particle (MIP) passing through the device. When this event happens, electron/holes pairs are produced and start drifting toward the electrodes. As a consequence the current signal shows a peak related the

amount of charge collected by the electrodes. Actually, the amount of collected charge strongly depends on the trap density.

Trap Type	E_C-E_{trap} (eV)	N_T (cm-3)	σ_n (cm-3)	σ_p (cm-3)
Donor	0.05	1E16	1E-13	1E-18
Donor	0.5	1E16	1E-15	1E-18
Acceptor	2.7	2E16	5E-16	1E-13

Table 1. Values for the Trapping and Recombination Centres implemented in TCAD environment.

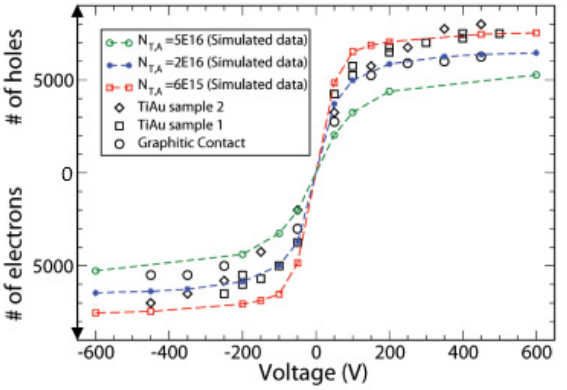

Fig. 9. Comparison between simulated charge collection and experimental measurements [11]

The comparison with experimental results is summarized in Fig. 9. Measured data related to different samples in terms of charge collection efficiency, i.e. the amount of collected charge, are reported along with simulation results. The overall agreement between simulations and actual measurements is good, assessing the suitability of the proposed modelling and simulation methodology and thus fostering the adoption of conventional VLSI TCAD tool for the design of innovative, diamond-based sensors.

5. Conclusions

The aim of this work was the development and validation of models and methodologies for device level simulation of diamond devices in commercial TCAD environment. To this purpose, a new custom-defined semiconductor material with the main parameters of polycrystalline CVD diamond has been added to the library of Synopsys Sentaurus TCAD. Moreover, an in-depth study of the effect of shallow and deep trap levels has been carried out, aiming at developing a suitable model for the diamond bandgap.

Steady-state and transient analyses have been carried out and compared with experimental results, aiming at validating the model. The overall agreement between simulations and actual measurements assesses the suitability of the proposed modelling and simulation methodology to reproduce the behavior of real devices. This foster its application as predictive tool for the optimization of innovative, diamond based electronics devices.

References

[1] Rashid et al., Numerical Parametrization of Chemical-Vapor-Deposited (CVD), polyCrystal Diamond for Device Simulation and Analysis, IEEE Trans. on Electron Dev., vol. 55, October 2008.
[2] J. Isberg, et al., High carrier mobility in single-crystal plasma-deposited diamond, Science, vol. 297, no. 5587, pp. 1670-1672, Sep. 2002.
[3] M. Brezeanu, Diamond Schottky Barrier Diodes, Ph.D. Thesis, Churchill College Dept. of Engineering, University of Cambridge, 2007.
[4] C. E. Nebel, M. Stutzmann, Transport properties of diamond: carrier mobility and resistivity, Handbook (Diamond and Rel.Mat.), May 2000.
[5] P.Y.Yu et al., Fundamentals of Semiconductors:Physics and Materials Properties, Berlin: Springer, 2nd ed., 1999.
[6] F. Maier, et al., Electron affinity of plasma-hydrogenated and chemically oxidized diamond (100) surfaces, Phys. Rev. B 64, 5 October 2001
[7] E. Borchi, et al., Model of carrier dynamics in chemical vapor deposition diamond detectors, Phys. Rev. B 71, 104103 – 3 March 2005.
[8] M. Bruzzi, et al., Defect analysis of a diamond detector by means of photoconductivity and thermal spectroscopy characterization, Phys. Stat. Sol. A 199, 138 (2003) 306, 308.
[9] C. Manfredotti, F. Wang, P. Polesello, E. Vittone, F. Fizzotti, A. Scacco, Appl.Phys. Lett. 67, 3376 (1995) 304, 308.
[10] S. Lagomarsino et al., Modelling of the Transport Properties of Diamond Radiation Sensors, Carbon Topics in Applied Physics, Volume 100, 2006, pp 303-327.
[11] S. Sciortino, Silicon On Diamond Detectors Project, Darmstadt, 2nd ADAMAS Workshop, GSI, Darmstadt 15-17 December, 2013.